15

Analysis of Infectious Mortality by Means of the Individualized Risk Model

Tatiana E. Sannikova

Institute of Numerical Mathematics, Moscow, Russia; tatiana@inm.ras.ru

Summary. The goal of this chapter is to describe the mechanism underlying the age-specific increase in death risk related to immunosenescence, to determine the cause-specific hazard rate as a function of immune system characteristics. A mathematical model that allows for the estimation of the age-specific risk of death caused by infectious diseases has been developed. The model consists of three compartments: (1) a model of immunosenescence, (2) a model of infectious disease, and (3) a model giving the relationship between disease severity and the risk of death. The proposed model makes it possible to analyze age-specific mortality from infectious diseases and to predict future changes in mortality due to public health activity. At the same time it can be used for individualized risk assessment.

Key words: Immune aging, pneumonia, mortality, antigenic load, infection rate, telomere.

15.1 Introduction

The age pattern of mortality from all causes has common traits for different human populations. These traits are relatively high during infancy and early childhood, very low during the reproductive period, increase exponentially from age 35 to 85, and decelerate at very old ages [11,25].

However, the detailed analysis of cause-specific mortality in countries with well-developed health care systems reveals that death rates from major causes do not follow this pattern [11,12]. For instance, death rates from malignant neoplasms rise at ages 30–54 years and decline afterwards. Mortality from parasitic infections is highest at ages 30–35 years [11]. It has been found that mortality from some cancers levels off around 85–90 years of age, followed by a plateau, or a decline in the last decades of life [4]. Steeply increasing after age 65 years are death rates from respiratory infections and cardiovascular diseases.

All this implies that different systems of the organism become vulnerable in different periods of life. One can suppose that excessive susceptibility to certain diseases or disorders occurs at a period of age-associated remodeling of the system [24].

We propose a new approach to estimate cause-specific risk of death. This approach is based on the modeling of physiological aging of the system responsible for the

lethal disease or disorders. There is some evidence that replicative senescence of T cells results in a growth of mortality caused by respiratory infections [1, 8]. Here we consider age-associated changes in the immune system and the way they influence the course and the outcome of respiratory infection. We develop a model of age-related risk of death from respiratory infections and make an attempt to fit data on pneumonia mortality in some countries.

15.2 Model of Age-Related Risk of Death from Respiratory Infections

The principal processes associated with immunosenescence are replacement of naive lymphocytes by memory cells and replicative senescence of lymphocytes. A decrease in the number of naive lymphocytes results in a weak and delayed immune response to new pathogens. Low replicative capacity of lymphocytes leads to a slowed immune response to any challenge as well. The slowed, inadequate immune responses accompanied by widespread damage of target tissues caused by pathogens. Damage of more than a third of vitally important organs (e.g., lung tissue in the case of pneumonia) is related with a high risk of death.

The relationship between immunosenescence and related mortality is represented by the model of age-related risk of death from respiratory infections (see Fig. 15.1). The model consists of three components: a model of immunosenescence [20], a model of infectious disease [13] and a relationship between disease severity and risk of death.

The first model, the mathematical model of immunosenescence, describes the age trend of immune system characteristics such as the concentration of naive and memory T cells and their replicative capacity. The model is represented by a system of ordinary differential equations (ODEs). Numerical solution of the system of ODEs yields the sets of immune characteristics for each age. These characteristics are used in the second model, the model of infectious disease, to determine the value of the lymphocyte concentration at the beginning of disease and the rate of immune response. This model makes it possible to simulate the course of unified infectious disease for each set of immune characteristics or, in other words, for each age. Disease severity is defined as a maximum of target tissue damage in the course of the disease.

The third model is a function of the distribution of resistance in the population, describing population heterogeneity in this characteristic. Infection resistance is defined as a probability of recovery at a certain value of target tissue damage (disease severity). As an output of the model we have risk assessment of lethal outcome in the course of the disease. To estimate the probability of death from certain diseases during a time interval (e.g., during one year) we multiply the risk of lethal outcome in the course of the disease by the probability of becoming infected during the interval under consideration.

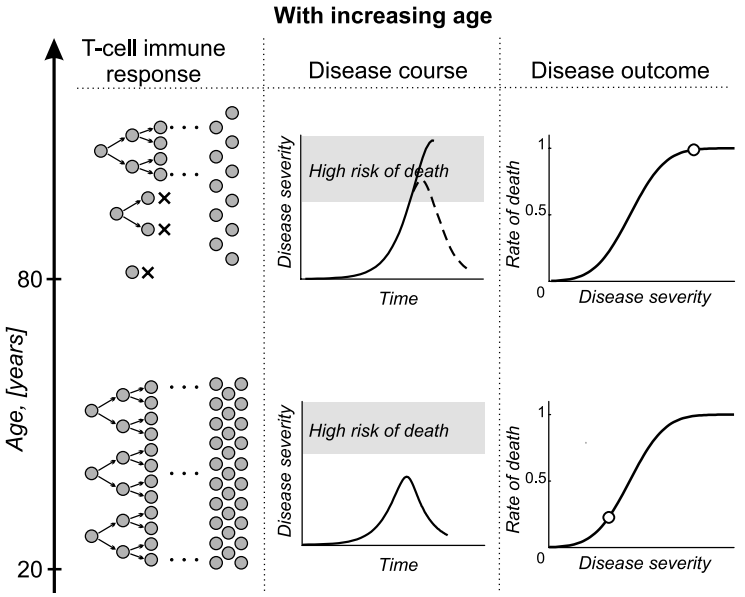

Fig. 15.1. The relationship between age-related changes in immune system and increasing risk of death from infectious disease. Proliferative capacity of T cells decreases with age, which results in deceleration of lymphocyte proliferation during immune response. So, the severity of the disease increases with increasing age. The higher the disease severity, the higher risk of lethal outcome.

15.2.1 Mathematical Model of Immunosenescence (M1)

The immune system undergoes significant changes in the course of life. According to the environmental challenges and mode of living, subsystems and organs of the immune system are either activated or suppressed. Obviously, the adaptive immune system undergoes more changes than the innate system. There is evidence that some components of the system of innate defense become even more active at older than at young ages. Changes in the population of B cells occur later and to a lesser extent. For simplicity, we consider age-related changes in the population of T cells.

The T cells can be broadly categorized as naive and memory. The specific immune system in the course of self-learning generates memory cells from naive cells. Memory cells are capable of providing a more rapid and effective immune response upon reencounter with antigens than their progenitors. With increasing age the number of memory cells increases, but the rate of naive lymphocyte production declines. So the immune system loses its ability to protect against new pathogens.

At the same time the proliferation potential of all immune cells is decreasing. In older individuals, 30–45% of lymphocytes cannot proliferate in response to antigenic stimuli [7]. Thus, the following processes determine age-related remodeling of the specific immune system: the replacement of naive cells by memory cells, replicative senescence of T cells, and a decrease in volume of lymphoid tissue.

The mathematical model of age-related changes in the immune system is represented by a system of ODEs. The choice of functional forms is based on the law of mass action. Variables of the model are

$N(\tau)$, the concentration of naive T cells in lymphoid tissue at age τ;
$M(\tau)$, the concentration of memory T cells in lymphoid tissue at age τ;
$P_N(\tau)$, the average length of telomere repeats in naive T cell at age τ;
$P_M(\tau)$, the average length of telomere repeats in memory T cell at age τ.

$$\frac{dN}{d\tau} = \frac{N^*}{V} - \alpha_1 \frac{L}{V} N - \mu_N N - \frac{dV}{d\tau}\frac{N}{V}, \tag{15.1}$$

$$\frac{dM}{d\tau} = \rho_1 \alpha_1 \frac{L}{V} N + \rho_2 \alpha_2 \frac{L}{V} M + \mu_M (M^* - N - M) - \frac{dV}{d\tau}\frac{M}{V}, \tag{15.2}$$

$$\frac{dP_N}{d\tau} = (P^* - P_N)\frac{N^*}{NV}, \tag{15.3}$$

$$\frac{dP_M}{d\tau} = \rho_1 \alpha_1 (P_N - P_M - \lambda_N)\frac{L}{V}\frac{N}{M} - (\rho_2 + 1)\alpha_2 \lambda_M \frac{L}{V}. \tag{15.4}$$

The first term in the first equation describes the influx of new naive T cells from the thymus. The rate of influx exponentially decreases with age,

$$N^*(\tau) = N_0^* e^{-k_T \tau}. \tag{15.5}$$

There is evidence that a T cell progenitor loses its proliferative capacity with age [17]. We assume that proliferative capacity is determined by the length of telomeric DNA. Here P^* is the telomere length in the cells which have recently left the thymus. It decreases with age as

$$P^*(\tau) = (P_0^* - P_{\min})e^{-k_P \tau} + P_{\min}. \tag{15.6}$$

Lymphoid tissue diminishes with age in both primary (thymus) and in peripheral immune organs (lymph nodes, spleen, and lymphoid tissues draining mucosal surfaces). The volume of the peripheral lymphoid tissue decreases with age as follows:

$$V(\tau) = (V_0 - V_{\min})e^{-k_V \tau} + V_{\min} \tag{15.7}$$

and compensates for the decline of the total number of T cells.

Initial conditions for system (15.1–15.7) are as follows:

$$N(\tau_0) = N^0; \qquad M(\tau_0) = M^0; \qquad P_N(\tau_0) = P_N^0; \qquad P_M(\tau_0) = P_M^0. \tag{15.8}$$

The physical meaning of model parameters and their estimates were discussed in detail in [20]. Initial conditions and estimates of parameters that allow simulating the normal aging of the immune system are givin in Table 15.1. Fig. 15.2 shows age trajectories of the model variables after 18 years. Regimes of normal, slowed, and accelerated immune aging were investigated in [20, 22]. The results of the simulations agree with the clinical observations and with the results of other models of immune processes [1,2,6,16].

Table 15.1. Initial conditions and model parameters for simulation of the normal aging of the immune system.

Parameter	Physical meaning and dimension	Estimate
α_1	Coefficient of sensitivity of naive T cells to antigen load (ml g^{-1})	$1.5 \cdot 10^4$
α_2	Coefficient of sensitivity of memory T cells to antigen load (ml g^{-1})	$1.5 \cdot 10^4$
μ_N	Death rate of naive T cells in the absence of antigen load (day^{-1})	$1.8 \cdot 10^{-4}$
μ_M	Death rate of memory T cells (day^{-1})	0.05
ρ_1	Number of memory T cells produced by one naive cell	100
ρ_2	Number of memory T cells produced by one memory cell	1.1
λ_N	Length of telomere repeats lost during transformation of naive cells to memory cell (bp $cell^{-1}$)	1400
λ_M	Length of telomere repeats lost during self-replication of memory cells (bp $cell^{-1}$)	500
M^*	Low limit for normal concentration of memory T cells in lymphoid tissue (cell ml^{-1})	$2.5 \cdot 10^9$
k_T	Rate of diminishing of naive T cell production with age (day^{-1})	$1.1 \cdot 10^{-4}$
k_V	Relative rate of reduction of lymphoid tissue volume with age (day^{-1})	$2.7 \cdot 10^{-5}$
k_P	Relative rate of the telomere repeats reduction in the progenitor of naive T cells (bp day^{-1})	$1 \cdot 10^{-5}$
L	Antigen load (g day^{-1})[1]	
N_0^*	The rate of T cell production by the thymus at the age of 18 (cell day^{-1})	$4 \cdot 10^8$
V_0	Volume of lymphoid tissue at the age of 18 (ml)	1500
$V_{\min}$	Minimal volume of lymphoid tissue (ml)	100
P_0^*	Length of telomere repeats in naive T cells produced at the age of 18 (bp $cell^{-1}$)	$8.3 \cdot 10^3$
$P_{\min}$	Minimal length of telomere repeats in the progenitor of naive T cells	100
N_0	The concentration of naive T cells at the age of 18 (cell ml^{-1})	$1.9 \cdot 10^9$
M_0	The concentration of memory T cells at the age of 18 (cell ml^{-1})	$6.45 \cdot 10^8$
P_{N0}	Length of telomere repeats in naive T cells at the age of 18	$8.8 \cdot 10^3$
P_{M0}	Length of telomere repeats in memory T cells at the age of 18	$7.4 \cdot 10^3$

[1] The value of antigenic load characterizes the influence of environmental and behavioral factors on immune system aging and can vary greatly in different individuals. For European populations it was estimated from 10^6 g day^{-1} to $2 \cdots 10^6$ g day^{-1}.

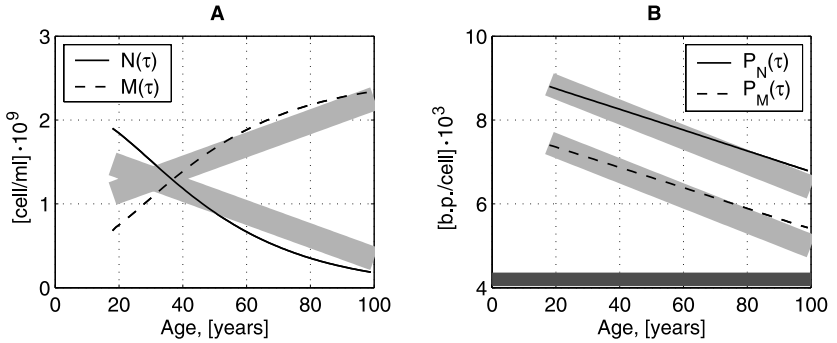

Fig. 15.2. Mathematical modeling of age-related changes in peripheral T cell population. (A) the dynamics of concentrations of naive ($N(\tau)$) and memory ($M(\tau)$) T cells in lymphoid tissue; (B) the dynamics of the telomere length in the naive ($P_N(\tau)$) and memory ($P_M(\tau)$) T cells. Wide grey strips depict variance of T cell concentrations and telomere lengths according to clinical observations [10,21]. Horizontal dark grey strip corresponds to the value of critical length for replicative senescence (known as the Hayflick's limit).

15.2.2 Model of Infectious Disease (M2)

A model of infectious disease is used to obtain the estimate of disease severity for age τ. The impact of different mechanisms on immune response in the course of pneumonia was studied [19], and it was shown that a decrease in T cell functioning is crucial for respiratory infections usually caused by an ubiquitous pathogen.

This mathematical model describes [13] the processes which determine the beginning, course, and outcome of all infections: invasion and propagation of the pathogen, infection-induced damage of tissues, immune response, elimination of the pathogen and tissue regeneration. The variables of the model are

$K(t)$, the concentration of the pathogen in target tissue;

$C(t)$, the concentration of specific lymphocytes in draining lymph nodes;

$F(t)$, the concentration of specific antibodies in blood;

$m(t)$, the fraction of target cells destroyed by pathogen.

The dynamics of the immune response is described by the system of four differential equations,

$$\frac{dK}{dt} = \beta K - \gamma F K, \tag{15.9}$$

$$\frac{dC}{dt} = \alpha(1-m)FK - \mu_c(C - C^*), \tag{15.10}$$

$$\frac{dF}{dt} = \rho C - \eta\gamma F K - \mu_f F, \tag{15.11}$$

$$\frac{dm}{dt} = \sigma(1-m)K - \mu_m m. \tag{15.12}$$

with the following initial conditions:

Table 15.2. Initial conditions and model parameters for simulation of infectious disease.

Parameter	Physical meaning and dimension	Estimate
β	Rate of pathogen propagation (day^{-1})	0.35
γ	Rate of pathogen neutralization by antibodies (ml pt^{-1} day^{-1})	$8.5 \cdot 10^{-14}$
α	Rate of specific lymphocyte proliferation (ml pt^{-1} day^{-1})	$5 \cdot 10^{-11}$
μ_C	Death rate of specific lymphocytes (day^{-1})	0.5
ρ	Rate of antibody production by lymphocytes (day^{-1})	$7 \cdot 10^3$
η	Number of antibodies required to neutralize one pathogen particle	20
μ_f	Death rate of specific antibodies (day^{-1})	0.05
σ	Rate of target organ damage by the pathogen (ml pt^{-1} day^{-1})	$9 \cdot 10^{-9}$
μ_m	Rate of target organ regeneration (day^{-1})	0.4
K_0	Infecting dose (pt ml^{-1})	10^3
C^*	The concentration of specific naive lymphocytes (cell ml^{-1})	—
C_m	The concentration of specific memory cells (cell ml^{-1})	—
k_1	The fraction of naive T cells involved in immune response	$1.5 \cdot 10^{-6}$
k_2	The fraction of memory T cells involved in immune response	$4.3 \cdot 10^{-4}$

$$K(t_0) = K_0; \quad C(t_0) = C_m + C^*; \quad F(t_0) = \frac{\rho(C_m + C^*)}{\mu_f}; \quad m(t_0) = 0. \quad (15.13)$$

To simulate the course of acute pneumonia we use initial conditions and parameter estimates given in Table 15.2 [19]. Note that the expression for initial value of specific lymphocytes contains the concentrations of naive lymphocytes C^* and memory cells C_m that are specific to the pathogen under consideration. We assume that the level of specific naive lymphocytes is homeostatic and in the case of natural death of lymphocytes only the excess (cloned) lymphocytes die (see the last term in equation 15.10).

The particular feature of the model of infectious disease is an equation for the dynamics of target tissue damage. Wide tissue damage causes loss of homeostasis and reduces lymphocyte proliferation (the first term in equation 15.10). This distinguishes this model from the models of immune-pathogen dynamics [18,26].

In clinical practice [15] a maximum of tissue damage is interpreted as disease severity S. In the case of pneumonia, damage to less than 15% of the cells of the three lower segments of the lung corresponds to mild disease with a low risk of death, damage to 35% of the cells of the three lower segments of the lung corresponds to medium severity with a death risk of 0.5, and disease with greater than 45% destroyed target tissue is defined as severe with a very high probability of death (≥ 0.77).

Varying the rate of immune response and initial concentration of specific lymphocytes according to the age trend we can simulate the course of infectious disease for different ages. It is assumed that the concentration of specific lymphocytes at the be-

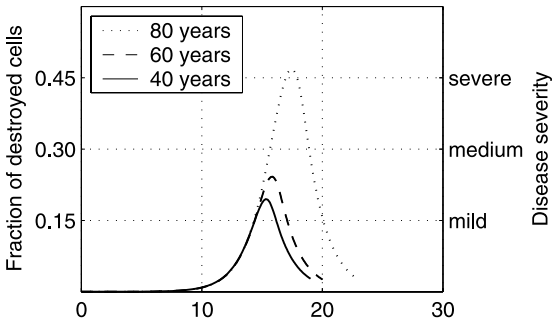

Fig. 15.3. The fraction of target cells destroyed by the pathogen in the course of disease for different ages (on the left vertical axis). Disease severity (on the right vertical axis). Disease severity is defined as a maximum of tissue damage.

ginning of the infection depends on the current concentrations of naive and memory T cells as follows:

$$C(t_0, \tau) = C^*(\tau) + C_m(\tau) = k_1 N(\tau) + k_2 M(\tau), \tag{15.14}$$

where t_0 denotes the time of the beginning of disease, τ denotes the age.

There is much evidence that the rate of lymphocyte proliferation decreases with age. Denote by α^0 the rate of specific lymphocyte proliferation at age 18 and by $\alpha(\tau)$ the rate at age τ. We assume that the ratio $\alpha(\tau)/\alpha^0$ is equal to the ratio of replicative capacity of T cells involved in the immune response at age τ to the one at age 18. The proliferative capacity of naive T cells involved in the immune response at age τ is defined by the concentration and the mean length of their telomeres $k_1 N(\tau)(P_N(\tau) - H)$. Here H is the Hayflick limit—the cell stops division when the telomere becomes shorter than H. The proliferative capacity of memory T cells can be represented in a similar manner. Then, the expression for $\alpha(\tau)$ is as follows:

$$\alpha(\tau) = \alpha^0 \frac{k_1 N(\tau)(P_N(\tau) - H) + k_2 M(\tau)(P_M(\tau) - H)}{k_1 N^0 (P_N^0 - H) + k_2 M^0 (P_M^0 - H)}, \tag{15.15}$$

where P_N^0, P_M^0, N^0, M^0 are values of the respective variables for the age of 18.

Note that the immune processes described in model (15.1)–(15.8) and in equation (15.10) are located in the lymph nodes, equation (15.9) represents changes of pathogen concentration in the target tissue, and equation (15.11) deals with antibody concentration in the blood. We consider variables located in different spatial compartments in order to use reasonable physical constants for modeling cell interaction. All transfer rates are included in the estimates for the rates of interactions (for details see [14]).

In Fig. 15.3 the trajectory of the disease severity is presented for three different ages. It is easy to see that in the interval from 60 to 80 years the severity of simulated disease increases approximately twofold. The higher the disease severity, the higher the risk of lethal outcome.

15.2.3 Relationship Between Disease Severity and the Risk of Death (M3)

In our context we define the infection resistance Res as a probability of recovery at value S of disease severity. Then, the probability of the lethal outcome is $p_L = 1 - Res$. Further, we assume that this characteristic is normally distributed in the population. Hence, the probability of the lethal outcome p_L at the severity value S could be represented as the corresponding distribution function

$$p_L(S) = \Phi(S) = \int_0^S \frac{1}{\sigma\sqrt{2\pi}} e^{(t-a)^2} dt. \tag{15.16}$$

The values of the parameter were estimated based on the clinical observations [15].

Thus, by means of the model of infectious disease and expression (15.16), a relationship between immunosenescence and the risk of death could be established. A constructed model of age-related risk of death from respiratory infections is represented by the flowchart in Fig. 15.4. It has two input parameters—antigenic load and the probability of becoming infected. As output it yields the probability of death from respiratory infections per year.

In the next section we attempt to apply this model to explain differences in pneumonia mortality observed in some developed countries.

15.3 Analysis of Pneumonia Mortality

The age patterns of mortality from respiratory infections share common traits in countries with well-developed health care systems. Generally, between ages 20 and 30 the probability of death from respiratory infections is minimal; sometimes it equals zero. The growth of the death rate begins after age 35. The death rates grow exponentially or almost exponentially after the age of 55 years.

WHO data on pneumonia mortality in Austria, Italy, Portugal, the United Kingdom, the USA, and Japan in 1999 are represented by symbols in Fig. 15.5. These

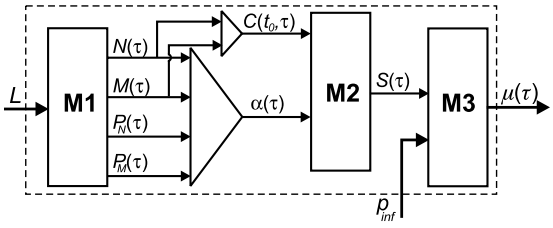

Fig. 15.4. Flowchart of the model of age-related risk of death from respiratory infections. **M1**, **M2**, and **M3** denote the model of immunosenescence, the model of infectious disease, and the relationship between disease severity and the risk of death, respectively. The model of age-related risk of death provides as an output mortality curve $\mu(\tau)$. The input parameters are antigenic load L and the probability of becoming infected p_{inf}.

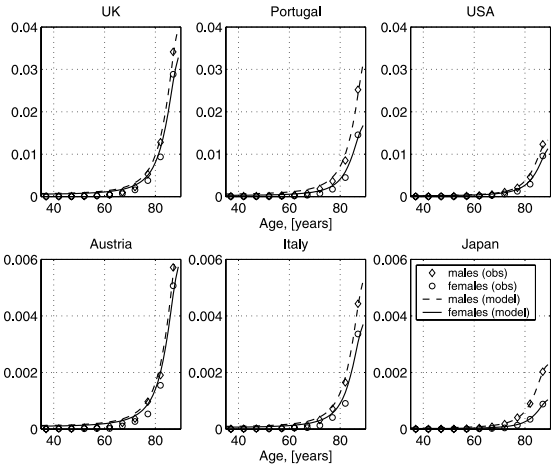

Fig. 15.5. Pneumonia mortality (probability of death from pneumonia per year) in Austria, Italy, Portugal, United Kingdom, USA, and Japan in 1999. WHO data are represented by symbols, results of simulation by lines.

countries were chosen because they use the same or coincident categories from the International Classification of Diseases (B-321, ICD-9; or J13, J14, J150–J159, ICD-10). Despite this, the probability of death from pneumonia in the age group 80–84 in the UK is 27 times higher than in Japan and 10 times higher than in Italy.

It could be suggested that higher mortality is associated with total health expenditure but this is not the case (Fig. 15.6). Moreover, life expectancy at birth does not reflect level of pneumonia mortality.

We assume that these populations experience different antigenic load throughout adult life. This can be related to differences in climatic and ecological conditions, modes of living, and national cuisines. We fit the model of age-related risk of death from respiratory infections to the data. The results of the simulations are represented by solid and dashed lines in Fig. 15.5. There is good agreement between the model

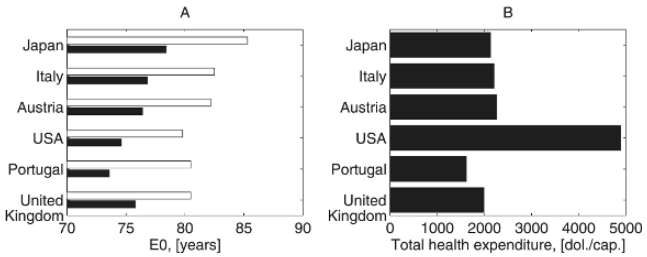

Fig. 15.6. (A) Life expectancy at birth (black bars correspond to males, white bars to females) and (B) total health expenditure in the countries under consideration [2000, WHO].

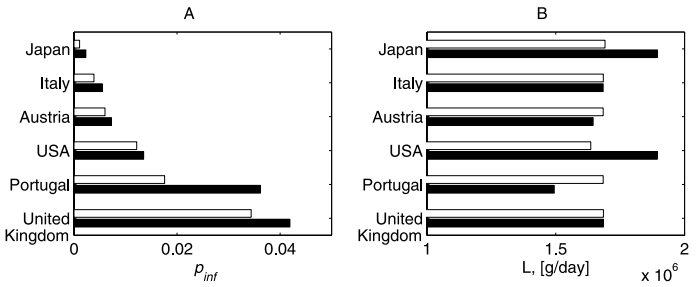

Fig. 15.7. Parameter estimates of environmental conditions which influenced immunosenescence in the populations under consideration. (A) Frequency of pneumonia and (B) antigenic load. Black bars correspond to males, white bars to females.

and the data sets for medium and large values of the death rate. For small values (age group 35–39), the estimated risk of death is higher than observed.

To provide a good fit, two parameters of the model were estimated for every population: antigenic load and the frequency of pneumonia (Fig. 15.7). Differences in age-specific mortality between countries are mainly described by variations in the parameter of frequency of pneumonia. Males in Japan and United States experienced a higher antigenic load than males in other countries under consideration. Probably, the higher rate of immunosenescence in the male populations of these countries was related to the dynamic and stressful mode of living [9,23].

15.4 Conclusions

The proposed model describes the relation between physiological and demographic aging. According to the proposed model, disease severity is determined by the concentrations of T cells and by the length of their DNA telomeres. After age 60, the course and outcome of infectious disease are highly influenced by the length of T cell telomeres. The existence of an association between higher risk of death from infectious disease and shorter telomere length has been shown [5]. This work describes the influence of heritable and environmental factors on immunosenescence and related mortality.

The values of immune system characteristics are assumed to be population average. In the case of availability of the clinical measurements, the proposed model is transformed into the individualized risk model, which makes it possible to predict consequences of some interventions. There is growing evidence that modification of the immune state by means of vaccination, antiviral and hormonal therapies, stem cell transplantation—and possibly by regulation of telomerase activity [3]—could slow down processes associated with immunosenescence.

In this chapter we demonstrate how this model can be used for analyzing pneumonia mortality. It also allows us to predict future changes in mortality due to public health activity.

Acknowledgments

The author thanks A.A. Romanyukha and A.I. Yashin for their attention and support. This work is supported by the Russian Foundation for Basic Research grant 04-01-00579a, by Research School Grant 2007-5-1.5-12-02-065) and by the Max Planck Institute for Demographic Research.

References

1. Aspinall, R.: Longevity and the immune response. Biogerontology, **1**, 273–278 (2000).
2. Aviv, A., Levy, D., Mangel, M.: Growth, telomere dynamics and successful and unsuccessful human aging. Mech. Ageing Dev., **124**, 829–837 (2003).
3. Bodnar, A. G., Ouellette, M., Frolkis, M., Holt, S. E., Chiu, C.-P., Morin, G. B., Harley, C. B., Shay, J. W., Lichtsteiner, S., Wright, W. E.: Extension of life-span by introduction of telomerase into normal human cells. Science, **279**, 349–352 (1998).
4. Caruso, C., Lio, D., Cavallone, L., Franceschi, C.: Aging, longevity, inflammation, and cancer. Ann. NY. Acad. Sci., **1028**, 1–13 (2004).
5. Cawthon, R. M., Smith, K. R., O'Brien, E., Sivatchenko, A., Kerber, R. A.: Association between telomere length in blood and mortality in people aged 60 years or older. Lancet, **361**, 393–395 (2003).
6. De Boer, R. J.: Mathematical model of human CD4+ T-cell population kinetics. The Netherlands Journal of Medicine, **60**, 17–26 (2002).
7. Effros, R. B.: Costimulatory mechanisms in the elderly. Vaccine, **18**, 1661–1665 (2000).
8. Effros, R. B.: T cell replicative senescence pleiotropic effects on human aging. Ann NY Acad Sci, **1019**, 123–126 (2004).
9. Epel, E. S., Blackburn, E. H., Lin, J., Dhabhar, F. S., Adler, N. E., Morrow, J. D., Cawthon, R. M.: Accelerated telomere shortening in response to life stress. PNAS, **101**, 17312–17315 (2004).
10. Fagnoni, F. F., Vescovini, R., Passeri, G., Bologna, G., Pedrazzoni, M., Lavagetto, G., Casti, A., Franceschi, C., Passeri, M., Sansoni, P.: Shortage of circulating naive CD8+ T cells provides new insights on immunodeficiency in aging. Blood, **95**, 2860–2868 (2000).
11. Horiuchi, S., Finch, C. E., Mesle, F., Vallin, J.: Differential patterns of age-related mortality increase in middle age and old age. J. Gerontol. A. Biol. Sci. Med. Sci., **58**, B495–507 (2003).
12. Horiuchi, S., Wilmoth, J.: Age patterns of the life table aging rate for major causes of death in Japan, 1951–1990. J Gerontol A Biol Sci Med Sci, **52**, B67–77 (1997).
13. Marchuk, G.: Mathematical modelling of immune response in infectious diseases. Kluwer Academic Publishers, Dordrecht (1997).
14. Marchuk, G., Romanyukha, A. A., Bocharov, G.: Mathematical model of antiviral immune response. II. Parameters identification of acute course of viral hepatitis B data. J. Theor. Biol., **151**, 41–70 (1991).
15. Marchuk, G. I., Berbentzova, E. P.: Acute pneumonia: immunology, severity assessment, clinic, treatment. Nauka, Moscow (1989) (in Russian).
16. Mariani, L., Turchetti, G., Franceschi, C.: Chronic antigenic stress, immunosenescence and human survivorship over the 3 last centuries: heuristic value of a mathematical model. Mech. Ageing Dev., **124**, 453–8 (2003).
17. Nikolich-Zugich, J.: T cell aging: naive but not young. J. Exp. Med., **201**, 837–840 (2005).

18. Nowak, M. A., May, R. M.: Virus Dynamics: Mathematical Principles of Immunology and Virology. Oxford University Press, Oxford (2000).
19. Romanyukha, A. A., Rudnev, S. G., Sidorov, I. A.: Energy cost of infection burden: An approach to understanding the dynamics of host–pathogen interactions. J. Theor. Biol., **241**, 1–13 (2006).
20. Romanyukha, A. A., Yashin, A.: Age related changes in population of peripheral T cells: towards a model of immunosenescence. Mech. Ageing Dev., **124**, 433–443 (2003).
21. Rufer, N., Brummendorf, T. H., Kolvraa, S., Bischoff, C., Christensen, K., Wadsworth, L., Schulzer, M., Lansdorp, P. M.: Telomere fluorescence measurements in granulocytes and T lymphocyte subsets point to a high turnover of hematopoietic stem cells and memory T cells in early childhood. J. Exp. Med., **190**, 157–168 (1999).
22. Sannikova, T. E., Rudnev, S. G., Romanyukha, A. A., Yashin, A. I.: Immune system aging may be affected by HIV infection: mathematical model of immunosenescence. Russian Journal of Numerical Analysis and Mathematical Modeling, **19**, 315–329 (2004).
23. Segerstrom, S. C., Miller, G. E.: Psychological stress and the human immune system: a meta-analytic study of 30 years of inquiry. Psychol. Bull., **130**, 601–630 (2004).
24. Ukraintseva, S. V., Yashin, A. I.: How individual age-associated changes may influence human morbidity and mortality patterns. Mech. Ageing Dev., **122**, 1447–1460 (2001).
25. Vaupel, J. W., Carey, J. R., Christensen, K., Johnson, T. E., Yashin, A. I., Holm, N. V., Iachine, I. A., Kannisto, V., Khazaeli, A. A., Liedo, P., Longo, V. D., Zeng, Y., Manton, K. G., Curtsinger, J. W.: Biodemographic trajectories of longevity. Science, **280**, 855–860 (1998).
26. Wigginton, J. E., Kirschner, D.: A model to predict cell-mediated immune regulatory mechanisms during human infection with *Mycobacterium tuberculosis*. J. Immunol., **166**, 1951–1967 (2001).